Second Harmonic Generation Phase Measurements of Cr(VI) at a Buried Interface

Amanda L. Mifflin, Michael J. Musorrafiti, Christopher T. Konek, and Franz M. Geiger*

Department of Chemistry and the Institute for Environmental Catalysis, Northwestern University, 2145 Sheridan Road, Evanston, Illinois 60208

Received: September 13, 2005

Surface second harmonic generation (SHG) phase measurements are carried out on methyl ester-functionalized fused quartz/water interfaces in the presence and absence of Cr(VI). The experiments are performed at pH 7, room temperature, and a chromate concentration of 10^{-4} M, which corresponds to monolayer Cr(VI) coverage. The liquid/solid interface is probed from the fused quartz side by directing the probe light field at 580 nm onto the interface together with an SHG reference signal at 290 nm that is collinear with the fundamental. The phase difference of the SHG signals generated at the interface in the presence and absence of Cr(VI) is 85 degrees, which is consistent with SHG resonance enhancement observed for the surface-bound Cr(VI) near 290 nm. The optical arrangement discussed here does not require vacuum technology or optics that compensate for the dispersion of the fundamental and the second harmonic E-fields in the two condensed-phase media. This approach is general and can be applied for analyzing thermodynamic and kinetic data derived from SHG measurements of physical and chemical processes occurring at any buried interface.

I. Introduction

Although the second-order susceptibility, $\vec{\chi}^{(2)}$, is a real number for a medium that is optically transparent at both the fundamental and the second harmonic frequencies, it is a complex number for a medium that can undergo light absorption at either of these frequencies.[1−3] As with all complex numbers, this means that there is a phase associated with the imaginary, resonant contribution to the second-order susceptibility, $\vec{\chi}^{(2)}_{R}$, that will differ from the real, nonresonant contribution, $\vec{\chi}^{(2)}_{NR}$. Determining the phase difference between the nonresonant and resonant second-order susceptibility is crucial for analyzing and interpreting kinetic, thermodynamic, and spectroscopic data obtained using nonlinear optics.[1−26] In the case of second harmonic generation (SHG), one or more electronic resonances, each with their individual phases, can interfere with the nonresonant second-order susceptibility, as well as with one another.[4,5,27−30] The phase difference is also important when the wavelength of the laser probe field is not exactly in but near resonance with an electronic transition, or when multilayer systems are studied where various layers can contribute to the SHG signal.

If a surface-bound chemical species that absorbs at the fundamental or at the second harmonic wavelength is present on an optically transparent substrate, the phase difference between the resonant and the nonresonant SHG contributions can be determined by interfering the SHG signal from the interface with an SHG signal generated by a nonlinear optical reference medium.[4,5] This interference experiment is carried out in the presence and absence of the adsorbed species and uses the nonlinear optical reference crystal in transmission geometry. When the reference SHG E-field is generated in the reference crystal, it is produced in phase with the incident fundamental E-field if the reference crystal possesses a positive second-order susceptibility far from electronic resonance.[1,3] If the residual fundamental E-field is then directed onto a second nonlinear optical medium, a second SHG E-field is produced. If the reference SHG E-field remains collinear with the residual fundamental E-field, the first and the second SHG E-fields will interact based on their relative phases (Figure 1).[4,5] One can alter the phase shift, $\Delta\gamma$, between the SHG E-fields from the two media by using the dispersion of light in air.[4,5] For the purpose of this work, this phase shift, $\Delta\gamma$, refers to the difference in phase between two SHG generating media separated by air, while the term phase difference, $\Delta\phi$, refers to the difference in phase between two components to the second-order susceptibility, i.e., $\vec{\chi}^{(2)}_{NR}$ and $\vec{\chi}^{(2)}_{R}$. Obtaining this phase difference, $\Delta\phi$, is the goal of the experiment.

Although dry air has an average refractive index of 1.0003 in the UV-visible region of the spectrum, the digits after the fourth decimal place vary with wavelength,[31] resulting in light at different frequencies traveling at different velocities. An important implication of this dispersion of light in air is that the first SHG E-field will undergo a phase shift with respect to the fundamental E-field traveling collinearly with this first SHG E-field.[4,5] Therefore, when the second SHG E-field is generated, it will have a phase that differs from the first SHG E-field. This phase shift causes the two SHG E-fields to interfere with one another.[4,5] The dispersion of light in air causes the phase shift, and varying the amount of air between the two SHG media will therefore vary the phase shift. This allows for the measurement of an oscillatory interference pattern.[4,5] This interference pattern can be described by a cosine function as follows:

$$I_{2\omega} = |E_1 + E_2 e^{i\Delta\gamma}|^2 = E_1^{\,2} + E_2^{\,2} + 2E_1E_2\cos(\Delta\gamma) \quad (1)$$

In eq 1, $I_{2\omega}$ is the total SHG intensity, and E_1 and E_2 are the SHG E-fields from medium 1 and medium 2.

Two experimental approaches, pioneered by Chang et al.[4] and by Kemnitz et al.,[5] have been utilized to quantify this phase shift by varying the quantity of air between two SHG media. Chang et al. placed the two nonlinear optical media a set distance apart in a vacuum chamber and gradually dosed dry air into the chamber, varying the pressure between 30 and 760 Torr. In

* To whom correspondence should be addressed. E-mail: geigerf@chem.northwestern.edu

10.1021/jp055174n CCC: $30.25
Published on Web 12/03/2005

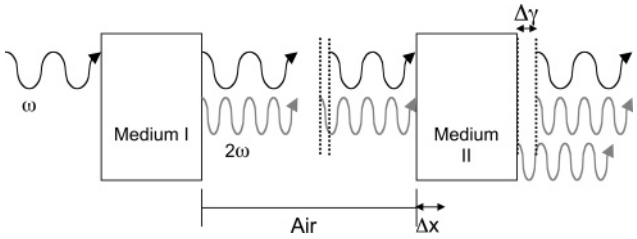

Figure 1. General principle for the appearance of phase shifts between two SHG media separated by air.

TABLE 1: Periods of Oscillation Calculated from Equation 4 and from Ciddor[32]

λ [nm]	$(n-1) \times 10^8$ [a]	2ω [nm]	Δn [a]	l_o [mm] [a]	l_o[mm] [b]
420	28175	210	3.571E−05	6	6
460	28016	230	2.783E−05	8	9
500	27896	250	2.250E−05	11	13
540	27803	270	1.866E−05	15	15
580	27728	290	1.578E−05	18	19
620	27669	310	1.353E−05	23	23
660	27620	330	1.175E−05	28	28
700	27579	350	1.032E−05	34	34
740	27545	370	9.13E−06	41	41
780	27516	380	8.15E−06	48	49

[a] Standard air: 0% RH and 300 ppm CO_2. [b] 45% RH and 450 ppm CO_2.

the method used by Kemnitz et al., the reference nonlinear optical medium was positioned after the surface of interest into the exigent beam path. By varying the distance between the nonlinear media, the experiment could be carried out in air at constant ambient pressure. The distance, l_o, over which the medium was moved in order to undergo one period of oscillation is given by:[5]

$$l_o = \frac{\lambda}{2\Delta n} \tag{2}$$

where λ is the wavelength of the fundamental probe E-field and Δn describes the dispersion of light due to air, given by $\Delta n = n_{2\omega} - n_{\omega}$.[5] The distances calculated from eq 2 for the visible region in standard air[31] and in air at 45% relative humidity,[32] the average relative humidity recorded in our laboratory, and 450 ppm CO_2,[32] common for major US city suburbs, are listed in Table 1. These methods are ideal for studying solid or liquid surfaces under a gas or a gas mixture such as air, but are not straightforward to implement for buried interfaces, such as solid/liquid or liquid/liquid interfaces. The approach of Chang et al. requires a vacuum chamber to control air pressure, which is not ideal for studying a liquid system. Applying the optical arrangement of Kemnitz et al. to a buried interface would require a realignment of the interfering nonlinear optical fields in front of the detector. This is due to the divergence of the SHG E-field from the sample and the fundamental E-field in the condensed phase as a result of optical dispersion. In this work, we show how the phase differences between $\vec{\chi}^{(2)}_{NR}$ and $\vec{\chi}^{(2)}_{R}$ can be determined at buried interfaces without the use of a vacuum system or the compensation for optical dispersion. This variation of the earlier pioneering SHG phase measurements can be carried out to determine the phase difference between resonant and nonresonant $\chi^{(2)}$ contributions at buried interfaces.

II. Phase Relations in SHG

We have previously shown that in the case of a first-order desorption process, the decay of the SHG E-field with respect to time depends on the phase difference between the $\vec{\chi}^{(2)}_{NR}$ and $\vec{\chi}^{(2)}_{R}$ contributions,[33] according to

$$\frac{|\vec{E}_{2\omega}|}{|\vec{E}_{\omega}|^2} \propto \sqrt{(\chi^{(2)}_{NR})^2 + \theta_o{}^2 N^2_{ML} e^{-2kt}\langle\alpha^{(2)}\rangle^2 + 2\chi^{(2)}_{NR}\theta_o N_{ML} e^{-kt}\langle\alpha^{(2)}\rangle\cos(\Delta\phi)} \tag{3}$$

In this equation, $\vec{E}_{\omega}$ is the pump electric field, $\vec{E}_{2\omega}$ is the generated second harmonic electric field, k is the desorption rate constant, θ_o is the initial relative surface coverage before desorption is initiated, N_{ML} is the absolute surface coverage in the monolayer regime, and $\langle\alpha^{(2)}\rangle$ is the molecular hyperpolarizability averaged over all molecular orientations. For phase differences ranging between 0° and 90°, the SHG E-field decays exponentially in time, albeit with observed rates that can change by up to 60% when starting the desorption process at monolayer coverage.[33] The effect is most dramatic when the phase difference approaches 180°, where the SHG E-field can temporarily decrease to levels below the nonresonant background level.[33] Clearly, a quantitative assessment of the phase difference can aid in the analysis of kinetic data.

The phase difference between $\vec{\chi}^{(2)}_{NR}$ and $\vec{\chi}^{(2)}_{R}$ can also impact the analysis of thermodynamic measurements regarding physical parameters such as equilibrium constants for reversible solute−surface interactions. For the Langmuir adsorption model, one can write

$$\frac{|\vec{E}_{2\omega}|}{|\vec{E}_{\omega}|^2} = \sqrt{(\chi^{(2)}_{NR})^2 + \left(\left(\frac{KC_{bulk}}{1+KC_{bulk}}\right)N_{ML}\langle\alpha^{(2)}\rangle\right)^2 + 2\chi^{(2)}_{NR}\left(\frac{KC_{bulk}}{1+KC_{bulk}}\right)N_{ML}\langle\alpha^{(2)}\rangle\cos(\Delta\phi)} \tag{4}$$

where C_{bulk} is the bulk solute concentration in solution and K is the equilibrium constant in units of M^{-1}. Figure 2A shows plots of eq 4 with $\vec{\chi}^{(2)}_{NR} = 50$, $N_{ML}\langle\alpha^{(2)}\rangle = 100$ and $K = 10^6$, referenced to the molarity of one liter of water, for phase differences of 0, 45, 90, 135, and 180 degrees. Clearly, the shapes of the isotherms depend on the assumed value of $\Delta\phi$. However, these differences may not be evident for $\Delta\phi$ values between 0 and 90 degrees when considering the scatter typically associated with SHG laboratory measurements. Nevertheless, the assumed value of $\Delta\phi$ impacts the equilibrium constant obtained from experimental SHG adsorption isotherms. Figure 2B shows that if $\Delta\phi$ is assumed to be zero during the analysis, the relative error introduced into the reported value for K can be as high as 40% when $\Delta\phi$ is, in reality, 90 degrees.

We have used the assumptions that $\Delta\phi = 0$ degrees and that $\Delta\phi = 90$ degrees to analyze thermodynamic and kinetic data of the environmental priority pollutant Cr(VI) interacting with functionalized fused quartz/water interfaces.[33,34] These studies were conducted with the goal of understanding how environmentally relevant organic adlayers influence the binding, and thus the transport and environmental fate, of hexavalent chromium on the molecular level.[33−37] However, knowing that the phase difference can have an impact on these analyses, we determined $\Delta\phi$ for Cr(VI) interacting with functionalized fused quartz/water interfaces and show here how these measurements can be carried out at liquid/solid interfaces.

III. Experimental Section

To carry out a phase measurement at a buried interface, one can place the reference nonlinear optical medium in the incident

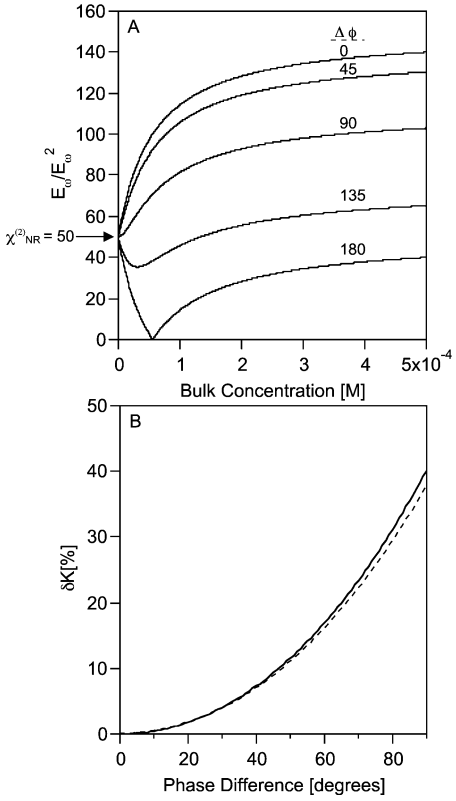

Figure 2. (A) Calculated SHG E-field as a function of bulk solution concentration for a Langmuir adsorption process with $K = 10^6$ for various phase differences between the resonant and nonresonant $\chi^{(2)}$ contribution. (B) Relative error in K due to uncertainties in $\Delta\phi$ assuming a phase difference of zero for $K = 10^6$ (dashed line) and 10^5(solid line). See text for details.

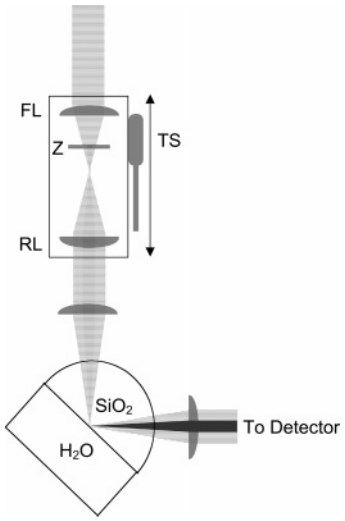

Figure 3. Optical setup for SHG phase measurements at buried interfaces. FL = focusing lens, z = z-cut quartz, RL = recollimating lens, TS = translational stage.

beam path, as shown in Figure 3. The fundamental probe E-field is partially focused into a z-cut quartz crystal of 1 mm thickness (Edmund Scientific), which acts as the reference nonlinear optical medium. The amplitude of the SHG reference E-field can be modulated by translating or rotating the crystal. The focusing lens, the z-cut quartz crystal, and the recollimating lens are placed onto an optical rail, which is bolted onto a translational stage with a 1 in. travel range. To vary the distance between the z-cut quartz and the buried interface, the translational stage is moved via a micrometer, thus moving the entire reference assembly. The remaining fundamental E-field and the SHG E-field exiting the reference assembly are collected using a recollimating lens and directed onto the interface of interest.

A detailed description of the synthetic procedures for the organosilanes and the surface functionalization has been given previously.[37,38] Methyl ester-functionalized silanes were freshly deposited on the flat side of a 1 in.-diameter fused quartz hemispherical lens (ISP Optics). The substrates with the ester-functionalized surfaces were stored in a closed beaker in air and rinsed twice with water maintained at pH 7 before bringing them in contact with the aqueous phase in the flow cell. Detailed characterization studies of the siloxane adlayers can be found elsewhere.[37,38]

The SHG experiments were conducted using a Teflon sample cell described in detail previously.[35,36] Briefly, after deposition of the siloxane adlayers, the functionalized lens was clamped leak-tight to the custom-built Teflon sample cell through a Viton O-ring. The sample cell was connected to Tygon tubing with Teflon fittings (Swagelok). The aqueous phase was injected using a syringe and a needle through a rubber septum, and the pH of the potassium chromate (ICN) solution and the aqueous phase was maintained at pH 7 using solutions of NaOH and HCl (Fisher).

The laser system used in these experiments, described in prior work,[35,36] consists of a Ti:sapphire laser (kHz, 120 fs, Hurricane, Spectra Physics) pumping an optical parametric amplifier (OPA-CF, Spectra Physics). The output light from the OPA at 580 nm was focused through the z-cut quartz assembly, recollimated, and then focused onto the aqueous/solid interfaces at an angle of 60° (spot size approximately 50 μm in diameter). Adsorbed Cr(VI) was monitored via a two-photon resonance centered around 290 nm. Based on previous results obtained at the fused quartz/water interface,[36] the enhancement of the SHG signal in the presence of Cr(VI) is consistent with the fundamental probe light being in resonance with ligand-to-metal charge-transfer transitions in the chromate ion. After isolating the SHG signal from processes other than SHG via Schott filters and a monochromator, the SHG signal was collected using a single-photon counting system.

IV. Results and Discussion

The first experiment carried out was a background measurement in order to determine if the reference assembly was well aligned with the fundamental E-field direction. In these experiments, we probed the methyl ester-functionalized fused quartz/water interface using a 45-in/s-out polarization combination to minimize the effect of surface roughness on the measurements. The reference assembly, with the z-cut quartz crystal removed, was translated in 0.183(3) cm increments over a range of 1.646-(3) cm. Figure 4 shows that the resulting SHG intensity remains approximately constant, indicating that motion of the focusing and recollimating lenses does not cause significant misalignment of the fundamental E-field at the interface. Also shown in Figure 4 are the results from the same experiment, but now with the z-cut quartz crystal present in the reference assembly. In the absence and presence of Cr(VI), the methyl ester-functionalized fused quartz/water interface exhibits oscillatory patterns that are offset in phase and in amplitude.

Figure 5 shows the baseline-subtracted SHG signal intensities for the absence and presence of a Cr(VI) monolayer at the methyl ester-functionalized fused quartz/water interface, and the results of fitting eq 1 to the data in the following form:

$$f(x) = y_o + A\cos(fx + \Delta\gamma) \quad (5)$$

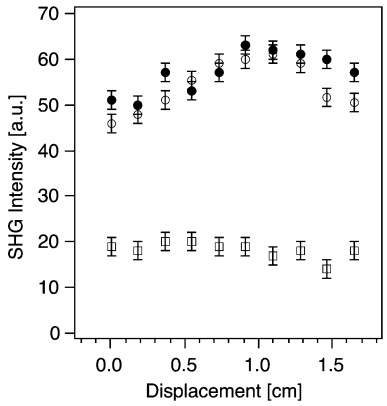

Figure 4. SHG response from a methyl ester-functionalized fused quartz/water interface maintained at pH 7 as a function of displacement on the reference assembly with z-cut quartz present for the absence (empty circles) and presence (filled circles) of Cr(VI) at the functionalized interface. SHG baseline response from a methyl ester-functionalized fused quartz/water interface maintained at pH 7 as a function of displacement on the reference assembly without z-cut quartz present (empty squares). Polarization combination was 45-in/s-out.

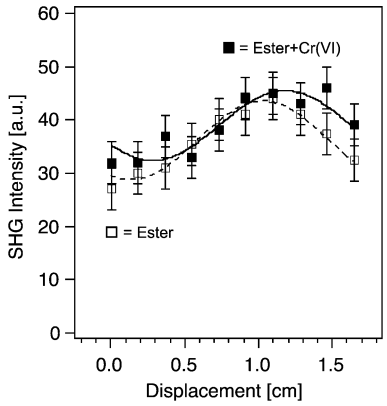

Figure 5. Baseline-subtracted data from Figure 4 for the absence (empty squares) and presence (filled squares) of Cr(VI) at the functionalized interface and fits to a cosine function for the absence (dashed line) and presence (solid line) of Cr(VI) at the interface. See text for details.

In eq 5, y_o is the sum of the SHG intensities from the z-cut quartz reference and the functionalized fused quartz/water interface, A is the amplitude of the interference pattern, and $\Delta\gamma$ is the phase shift between the z-cut quartz reference and the ester-functionalized surface (no Cr(VI) present) or the ester-functionalized surface with adsorbed Cr(VI) present. The frequency of the SHG E-field in air is given by $f = 2\pi/l_o$ and is held constant at 3.5 cm^{-1} for air at zero percent relative humidity. The fits reveal phase shifts between the z-cut quartz reference and the ester-functionalized surface in the presence and absence of adsorbed Cr(VI) of 123(11) degrees and of 152(5) degrees, respectively. These phase shifts increase by 11 degrees when using a value for f of 3.3 cm^{-1} in the fits to the data shown in Figure 5. This value for f was obtained when considering the dispersion of light in air at a relative humidity of 45%, 450 ppm of CO_2 and 74 degrees F.[32]

To obtain the phase difference between the Cr(VI) SHG signal, $\vec{\chi}^{(2)}_R$, and the SHG signal from the functionalized fused quartz/water interface, $\vec{\chi}^{(2)}_{NR}$, a vector analysis is carried out. The SHG signal from the functionalized fused quartz/water interface with no Cr(VI) present is used as the reference point for this analysis. Thus, the Cartesian coordinates of the vector used in the analysis are $x_{ester} = 1$ and $y_{ester} = 0$. We are then able to obtain, in two steps, a vector for the signal while Cr(VI) is present at the ester-functionalized interface in this coordinate system. In step one, the ratio of the combined signal from adsorbed Cr(VI) and the interface to the signal from the plain ester-functionalized fused quartz/water interface (no Cr(VI) present) was determined to be 1.2 through additional adsorption studies. In step two, the difference in the phase shifts between the z-cut quartz reference and the functionalized interface in the presence and absence of chromate, i.e., $\delta\Delta\gamma = \Delta\gamma_{Cr+ester} - \Delta\gamma_{ester}$, were calculated. This difference is -29 degrees, with a range of -13 degrees to -44 degrees. The resulting vector is given by the Cartesian coordinates $x_{Cr+ester} = 1.049$ and $y_{Cr+ester} = -0.582$. The difference between the unity vector for the ester system and the vector for the Cr+ester system is calculated to be $x = 0.049$ and $y = -0.582$ (this subtraction is depicted graphically in Figure 6). The angle between the unity vector for the ester system, i.e., the x-axis in this coordinate system, and the Cr-only vector is given by $\Delta\phi = \tan(\Delta y/\Delta x)$, where $\Delta x = x_{Cr+ester} - x_{ester}$ and $\Delta y = y_{Cr+ester} - y_{ester}$. The resulting phase difference between the SHG contributions, $\vec{\chi}^{(2)}_{NR}$ and $\vec{\chi}^{(2)}_R$, is 85 degrees, which is near the 90 degree phase difference typically associated with resonantly enhanced SHG signals.[1,3] The uncertainty in the phase difference is -27 degrees and $+14$ degrees, i.e., -35% and $+10\%$, as indicated by the gray area in Figure 6. When this analysis is carried out using air at 45% RH, we obtained a phase difference of 88 degrees, with uncertainties of -22 degrees and $+13$ degrees. It is important to note that the data analysis presented here does not yield the absolute phase, but only the phase difference between $\vec{\chi}^{(2)}_{NR}$ and $\vec{\chi}^{(2)}_R$ for the Cr(VI) adsorbed to the ester functionalized interface.

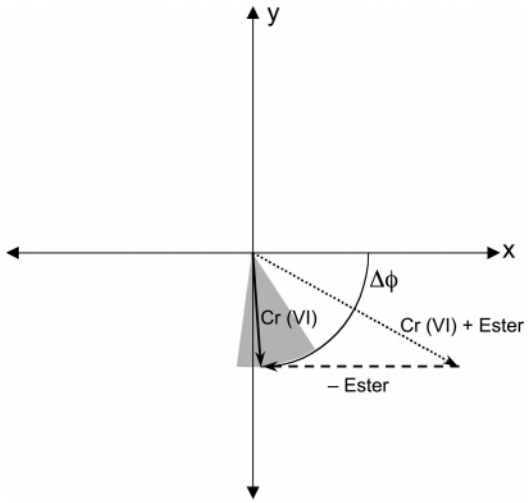

Figure 6. Diagram depicting the vector subtraction used to obtain the Cr(VI)-only vector (solid vector) from the Cr(VI) + interface vector (dotted vector) in coordinates based on the interface only vector (negative of which is the dashed vector). The gray area indicates the uncertainty in the phase difference.

The SHG spectrum of Cr(VI) adsorbed at the ester-functionalized fused quartz/water interface was recorded to verify resonance enhancement of the SHG signal at the wavelength used for the phase measurements discussed above. After recording the background signal from the ester-functionalized fused quartz/water interface, a 10^{-4} M Cr(VI) solution was introduced into the sample cell at pH 7 using the dual-pump flow setup described in our previous work.[35] Based on our previous adsorption isotherm measurements, this Cr(VI) concentration results in monolayer coverage.[34] The SHG signal intensity was recorded for approximately 100 seconds once the Cr(VI) adsorption process had reached steady state. After 100

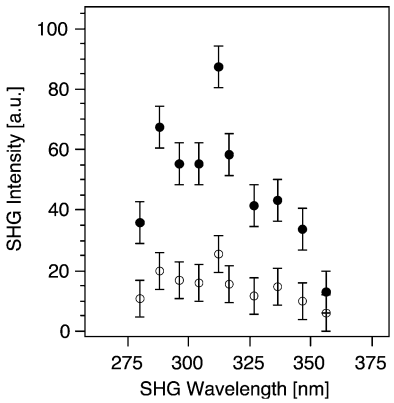

Figure 7. SHG spectrum obtained from the ester-functionalized fused quartz/water interface maintained at pH 7 in the absence (empty circles) and presence (filled circles) of Cr(VI).

seconds of data collection time, the Cr(VI) flow was turned off and water at pH 7 was used to flush the system. This sequence was repeated at various SHG wavelengths between 280 and 360 nm, resulting in SHG spectra for the interface both in the presence and absence of Cr(VI) (Figure 7). This procedure ensured that the functionalized quartz/water interface was exposed to Cr(VI) for a short enough period of time to avoid adlayer damage.[34] The experiments were carried out on two samples and the results were then signal-averaged. The resulting Cr(VI) SHG spectrum is consistent with resonantly enhanced SHG signals from Cr(VI) at the ester-functionalized fused quartz/water interface near 290 nm. The spectral dependence of the SHG signal is comparable to that obtained from Cr(VI) adsorbed at the fused quartz/water interface (no ester present).[36] This, in turn, is consistent with the phase difference of 85 degrees that we determined in the SHG interference studies.

Summary

In conclusion, we have presented how SHG phase measurements can be carried out at interfaces buried between two condensed-phase media. The optical arrangement discussed here does not require vacuum technology or optics that compensate for the dispersion of the fundamental and the second harmonic E-fields in the two condensed-phase media. Rather, the buried interface is probed by directing the fundamental E-field at frequency ω onto the interface together with an SHG reference signal at frequency 2ω that is collinear with the fundamental on the incident side. A focusing and recollimating assembly controls the SHG reference E-field amplitude and allows for the determination of the phase difference between the nonresonant and the resonant contributions to the second-order susceptibility of fused quartz/water interfaces functionalized with methyl ester-terminated siloxanes in the presence and absence of Cr(VI). The phase difference of the SHG signals generated at the interface in the presence and absence of Cr(VI) is around 90 degrees, which is consistent with SHG resonance enhancement observed for the surface-bound Cr(VI) between 290 and 320 nm. This work is important for analyzing thermodynamic and kinetic data derived from SHG measurements of physical and chemical processes occurring at buried interfaces. This method can also be applied to experiments where the incident laser probe field is limited to constant wavelength and not exactly on electronic resonance, if multiple closely spaced electronic resonance contribute to the SHG response, or if multilayer systems are studied in which the nonlinear optical response of the various layers can contribute to the SHG signal.

Acknowledgment. The authors would like to acknowledge helpful discussions with Professor Garth Simpson (Purdue University). We are grateful for donations and the technical support of Spectra Physics and CVI Lasers. A.L.M. gratefully acknowledges a Science To Achieve Results (STAR) graduate student fellowship from the EPA. Financial support for this work was provided by the NSF Experimental Physical Chemistry program (CAREER Award CHE-0348873).

References and Notes

(1) Shen, Y. R. *The Principles of Nonlinear Optics*; John Wiley & Sons: New York, 1984.
(2) Heinz, T. F. *Nonlinear Surface Electromagnetic Phenomena*; Elsevier: Amsterdam, 1991.
(3) Boyd, R. W. *Nonlinear Optics*; Academic Press: New York, 1992.
(4) Chang, R. K.; Ducuing, J.; Bloembergen, N. *Phys. Rev. Lett.* **1965**, *15*, 6.
(5) Kemnitz, K.; Bhattacharyya, K.; Hicks, J. M.; Pinto, G. R.; Eisenthal, K. B.; Heinz, T. F. *Chem. Phys. Lett.* **1986**, *131*, 285−290.
(6) Eisenthal, K. B. *Chem. Rev.* **1996**, *96*, 1343−1360.
(7) Walker, R. A.; Conboy, J. C.; Richmond, G. L. *Langmuir* **1997**, *13*, 3070−3073.
(8) Walker, R. A.; Gruetzmacher, J. A.; Richmond, G. L. *J. Am. Chem. Soc.* **1998**, *120*, 6991−7003.
(9) Walker, R. A.; Smiley, B. L.; Richmond, G. L. *Spectroscopy* **1999**, *14*, 18−29.
(10) Petralli-Mallow, T. P.; Plant, A. L.; Lewis, M. L.; Hicks, J. M. *Langmuir* **2000**, *16*, 5960−5966.
(11) Richter, L. J.; Petralli-Mallow, T. P.; Stephenson, J. C. *Opt. Lett.* **1998**, *23*, 1594−1596.
(12) Steel, W. H.; Damkaci, F.; Nolan, R.; Walker, R. A. *J. Am. Chem. Soc.* **2002**, *124*, 4824−4831.
(13) Zhang, X.; Esenturk, O.; Walker, R. A. *J. Am. Chem. Soc.* **2001**, *123*, 10768−10769.
(14) Zhang, X. C.; Walker, R. A. *Langmuir* **2001**, *17*, 4486-4489.
(15) Allen, H. C.; Gragson, D. E.; Richmond, G. L. *J. Phys. Chem. B* **1999**, *103*, 660−666.
(16) Baldelli, S.; Schnitzer, C.; Campbell, D. J.; Shultz, M. J. *J. Phys. Chem. B* **1999**, *103*, 2789−2795.
(17) Wei, X.; Miranda, P. B.; Shen, Y. R. *Phys. Rev. Lett.* **2001**, *86*, 1554−1557.
(18) Hommel, E. L.; Allen, H. C. *Anal. Sci.* **2001**, *17*, 137−139.
(19) Hommel, E. L.; Ma, G.; Allen, H. C. *Anal. Sci.* **2001**, *17*, 1325−1329.
(20) Shen, Y. R. *Nature* **1989**, *337*, 519−525.
(21) Shen, Y. R. *Surf. Sci.* **1994**, *299/300*, 551−562.
(22) Eisenthal, K. B. Equilibrium and dynamic processes at interfaces by second harmonic and sum frequency generation. In *Annual Review of Physical Chemistry*; Strauss, H. L., Babcock, G. T., Leone, S. R., Eds.; Annual Reviews Inc: Palo Alto, CA, 1992; Vol. 43; pp 627−661.
(23) Heinz, T. F.; Tom, H. W. K.; Shen, Y. R. *Phys. Rev. A* **1983**, *28*, 1883−1885.
(24) Simpson, G. J.; Rowlen, J. L. *Anal. Chem.* **2000**, *72*, 3407−3411.
(25) Simpson, G. J.; Rowlen, J. L. *Anal. Chem.* **2000**, *72*, 3399−3406.
(26) Baldelli, S.; Markovic, N.; Ross, P.; Shen, Y. R.; Somorjai, G. *J. Phys. Chem. B* **1999**, *103*, 8920−8925.
(27) Steel, W. H.; Walker, R. A. *Nature* **2003**, *424*, 296.
(28) Steel, W. H.; Walker, R. A. *J. Am. Chem. Soc.* **2003**, *125*, 1132−1133.
(29) Petersen, P. B.; Saykally, R. J.; Mucha, M.; Jungwirth, P. *J. Phys. Chem. B* **2005**, *109*, 10915−10921.
(30) Petersen, P. B.; Saykally, R. J. *J. Phys. Chem. B.* **2005**, *109*, 7976−7980.
(31) *CRC Handbook of Chemistry and Physics*, 71st ed.; Lide, D. R., Ed.; CRC Press: Boston, 1990−1991.
(32) Ciddor, P. E. *Appl. Opt.* **1996**, *35*, 1566−1573.
(33) Al-Abadleh, H. A.; Mifflin, A. L.; Musorrafiti, M. J.; Geiger, F. M. *J. Phys. Chem. B* **2005**, *109*, 16852−16859.
(34) Al-Abadleh, H. A.; Mifflin, A. L.; Bertin, P. A.; Nguyen, S. T.; Geiger, F. M. *J. Phys. Chem. B* **2005**, *109*, 9691−9702.
(35) Mifflin, A. L.; Gerth, K. A.; Geiger, F. M. *J. Phys. Chem. A* **2003**, *107*, 9620−9627.
(36) Mifflin, A. L.; Gerth, K. A.; Weiss, B. M.; Geiger, F. M. *J. Phys. Chem. A* **2003**, *107*, 6212−6217.
(37) Al-Abadleh, H. A.; Voges, A. B.; Bertin, P. A.; Nguyen, S. T.; Geiger, F. M. *J. Am. Chem. Soc.* **2004**, *126*, 11126−11127.
(38) Voges, A. B.; Al-Abadleh, H. A.; Musorrafiti, M. J.; Bertin, P. A.; Nguyen, S. T.; Geiger, F. M. *J. Phys. Chem. B.* **2004**, *108*, 18675−18682.